NUKLEONIKA 2016;61(2):169–177
doi: 10.1515/nuka-2016-0029

ORIGINAL PAPER

DE GRUYTER
OPEN

The experimental and theoretical investigations of damage development and distribution in double-forged tungsten under plasma irradiation-initiated extreme heat loads

Berit Väli, Tõnu Laas, Jana Paju, Veroonika Shirokova, Marian Paduch, Vladimir A. Gribkov, Elena V. Demina, Valeri N. Pimenov, Vadym A. Makhlaj, Maksim Antonov

Abstract. The influence of extreme heat loads, as produced by a multiple pulses of non-homogeneous flow of slow plasma (0.1–1 keV) and fast ions (100 keV), on double-forged tungsten (DFW) was investigated. For generation of deuterium plasma and fast deuterons, plasma-focus devices PF-12 and PF-1000 are used. Depending on devices and conditions, the power flux density of plasma varied in a range of 10^7–10^{10} W/cm^2 with pulse duration of 50–100 ns. Power flux density of fast ions was 10^{10}–10^{12} W/cm^2 at the pulse duration of 10–50 ns. To achieve the combined effect of different kind of plasmas, the samples were later irradiated with hydrogen plasma (10^5 W/cm^2, 0.25 ms) by a QSPA Kh-50 plasma generator. Surface modification was analysed by scanning electron microscopy (SEM) and microroughness measurements. For estimation of damages in the bulk of material, an electrical conductivity method was used. Investigations showed that irradiation of DFW with multiple plasma pulses generated a mesh of micro- and macrocracks due to high heat load. A comparison with single forged tungsten (W) and tungsten doped with 1% lanthanum-oxide (WL10) reveals the better crack-resistance of DFW. Also, sizes of cells formed between the cracks on the DFW's surface were larger than in cases of W or WL10. Measurements of electrical conductivity indicated a layer of decreased conductivity, which reached up to 500 μm. It depended mainly on values of power flux density of fast ions, but not on the number of pulses. Thus, it may be concluded that bulk defects (weakening bonds between grains and crystals, dislocations, point-defects) were generated due to mechanical shock wave, which was generated by the fast ions flux. Damages and erosion of materials under different combined radiation conditions have also been discussed.

Key words: divertor material • nuclear fusion • off-normal events • thermal shock • tungsten

B. Väli, T. Laas✉, J. Paju, V. Shirokova
School of Natural Sciences and Health,
Tallinn University, 10120 Tallinn, Estonia,
Tel.: +372 640 9404, Fax: +372 640 9118,
E-mail: tonu.laas@tlu.ee

M. Paduch
Institute of Plasma Physics and Laser Microfusion
23 Hery Str., 01-497 Warsaw, Poland

V. A. Gribkov
Institute of Plasma Physics and Laser Microfusion
01-497 Warsaw, Poland
and A. A. Baikov Institute of Metallurgy and Material Science RAS, Moscow 119991, Russia
and A. Salam International Centre for Theoretical Physics, I-34151 Trieste, Italy

E. V. Demina, V. N. Pimenov
A. A. Baikov Institute of Metallurgy and Material Science RAS, Moscow 119991, Russia

V. A. Makhlaj
Institute of Plasma Physics, NSC KIPT,
61108 Kharkov, Ukraine

M. Antonov
Faculty of Mechanical Engineering,
Tallinn University of Technology, Tallinn 19086, Estonia

Introduction

The construction and building of a number of large fusion facilities – tokamaks (ITER), stellarators (Wendelstein 7-X), inertial confinement devices (NIF, LMJ) – is in progress or already completed. Many of the basic problems that have been investigated and solved are in common for all fusion facilities [1, 2]. One aspect of the problems relevant to all future fusion devices is closely related to materials science. The main questions are: (1) how can the long-lasting irradiation and the heat loads that are generated in the fusion devices affect the plasma-facing materials; (2) why do the defects (e.g. mesh of cracks, pores, wave-like structures, exfoliations, bubbles, etc.) form, both on the irradiated materials surface and also in the bulk of the material.

In construction of magnetic confinement fusion facilities, tungsten (W) is currently considered as the most perspective material for use as a plasma-facing component due to its high melting point,

Received: 25 September 2015
Accepted: 2 December 2015

detachment properties, and low retention of D and T [3, 4]. Nevertheless, tungsten has several disadvantages, which may limit the use of it as an armour material – brittleness, poor creep strength and re-crystallisation. Therefore, a number of investigations were performed to determine whether dispersing tungsten with different oxides (e.g. La_2O_3, Y_2O_3, TiO, etc.) or other elements (Ta, Ti) might improve the physical properties of the alloy [5–10]. Different investigations have shown that while improving some of the tungsten's properties, adding the components can also lead to generation of tungsten dust to plasmas. Therefore, at least by now, the improvement of tungsten, by addition of different components, has not lead to significant improvement of all the necessary properties needed to develop a suitable divertor material. This makes it worth investigating other tungsten grades, which are either produced in other ways or differ by doped materials. One of the possible candidates for this is double-forged tungsten (DFW). The aim of double forging was to use densification process to yield an isotropic material. Due to manufacturing process disc-like shaped grains laid parallel to the surface [11]. DFW has a lower anisotropy, greater hardness than single-forged tungsten, therefore the strain-hardening behaviour was indicated [11]. Though, it should be noted that actually the densification was found only on edges of the material and porosity was increased in bulk [12].

Today, different devices are used for investigating effects of particles and heat loads on the material: pulsed lasers, electron beam facilities (in JUDITH 1 and 2), ion beam test facilities (in MARION and GLADIS) and plasma generators (in Pilot-PSI, Magnum-PSI, QSPA Kh-50, PISCES, etc.). However, there are no devices that can generate either the flux of particles (D, T, electrons, neutrons) or the heat loads with the identical parameters (i.e. power flux density q, duration of impulse τ, energy and density of plasma particles, etc.) to the most violent events of ITER. Therefore, it is of utmost importance to carry out experiments for obtaining data on plasma-materials interaction with different plasma-generating devices, with the aim of characterising the materials' behaviour in various events.

One of the effects that can be observed on the plasma-irradiated samples is the generation of the cracks on the materials' surface, which occurs due to thermal expansion and generation of thermal stresses during the heating-cooling cycles during irradiation of the sample. The rise of the samples' surface temperature also creates other defects, such as vaporisation and ablation of melted or semi-melted material. Thus, occurrence of surface damages is proportional to the rise of the surface temperature. Solving the 1D heat equation for homogeneous finite-duration heat loads on semi-infinite surface enables to calculate the maximal rise of the materials surface temperature as follows:

$$\Delta T \approx 2 \cdot q \sqrt{\frac{\tau}{\pi \cdot \rho \cdot \lambda \cdot c'}} \quad (1)$$

where q is power flux density, τ the influence time of the heat flux (plasma flux), ρ the material's density, λ the thermal conductivity and c the specific heat capacity (at constant pressure).

Since the materials' thermal conductivity and specific heat capacity depend on temperature, Eq. (1) cannot be used for exact determination of temperature rise due to heat flow. However, the occurrence of damage due to thermal loads is related with the heat flux factor (or heat damage factor) F. This factor, defined as $F = q \cdot \tau^{1/2}$, is proportional to the temperature increase, as shown in Eq. (1). This relation has been used as an indicator of thermal shock damage for graphite [13]. The heat flux factor can also be used for characterising plasma heat loads on materials in general [14], or specifically for tungsten [7, 11]. Varying the influence time of heat flow and power flux densities during experiments on different devices allows to obtain the values of the heat flux factor predicted for off-normal events on ITER. The approximate heat flux factors can be found for: (a) edge-localised modes (ELMs) – 2–6 $kW \cdot s^{1/2}/cm^2$, (b) vertical displacement events (VDEs) – 60 $kW \cdot s^{1/2}/cm^2$ and (c) disruptions – 10–20 $kW \cdot s^{1/2}/cm^2$ [4]. These heat flux factors are similar for plasma pulses generated by plasma-focus (PF) devices PF-12 and PF-1000, and by the plasma accelerator QSPA Kh-50.

Experimental set-up

For generation of heat loads in the PF-12 and PF-1000 devices, an influence of plasma (of energy equal to 0.1–1 keV) and fast ions (100 keV) was investigated (see e.g. [15] for a general review of PF devices). It is known that changing the distance between the anode and the sample (see Fig. 1) allows one to change plasma parameters on the sample surface [16, 17] (see also [18, 19] for an overview of PF-1000 and [10] for PF-12).

Experimental conditions in the PF-12 device at Tallinn University were as follows. The initial pressure of deuterium was approximately 8.5 Torr, capacitors voltage 20 kV, the maximum current 210–230 kA and current rise time 2.1 μs. It should here be noted that initial pressure of deuterium in some experiments (series of 25 plasma shots) was about 4–4.5 Torr, while the maximum current was 190–200 kA and current rise time 1.6 μs. Thus, the power flux density of slow plasma is almost the same for all the samples those were placed at the same distance from the anode.

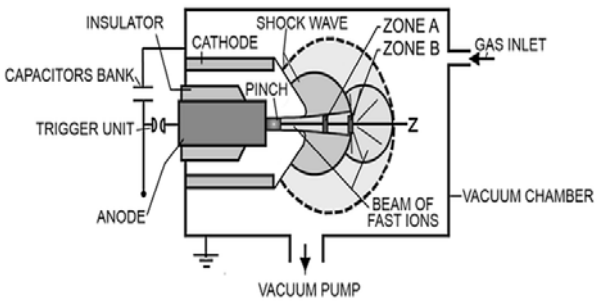

Fig. 1. Experimental set-up. The sample for plasma-ion irradiation is located on the holder at 3.5 cm (zone A) or 6.5 cm (zone B) from the anode.

The power flux density of slow plasma ($E \sim 0.1$–1 keV) and fast ions ($E \sim 100$ keV) was calculated considering initial conditions and plasma properties (velocity of a plasma shock wave and the current rise time) for working PF devices [16, 18, 19]. The power flux density of non-homogeneous slow plasma ($E \sim 0.1$–1 keV) varied from 5×10^7 to 5×10^9 W/cm^2 with interaction time equal to 50–100 ns depended on samples' positions. The power flux density of fast ions varied from 10^{10} to 10^{11} W/cm^2 during 10–30 ns interaction time. Preliminary calorimetric measurements at the PF-12 device showed that actually only 10–25% of plasma heat energy (less than 10% at sample distance 6.5 cm from the anode, and about 20% at distance 3.5 cm) was loaded upon the material surface. Therefore, the actual heat load factor of plasma at the PF-12 varied in the range of 3–10 kW·s$^{1/2}$/cm^2. Plasma and ion flux parameters generated at the PF-1000 were measured by different direct methods (see e.g. [18, 19]). It was estimated that hot plasma power flux density was 10^9 to 10^{10} W/cm^2 at the pulse duration ≥100 ns. For fast ions, the power flux density was 10^{11}–10^{12} W/cm^2 at the pulse duration ≤50 ns.

In zone A (see Fig. 1), the samples were affected first by streams of hot plasma of energy 0.1–1 keV, and afterwards by fast ion flows with energy of about 100 keV [15–17]. In zone B, the plasma stream and fast deuterons could reach the sample simultaneously. To understand completely the physical processes and the cause of damages during the irradiation, it should be noted that after the interaction between initial plasma and solid sample, some secondary tungsten plasma is formed in front of the samples' surface. Measurements in the PF-1000 showed that the temperature of the secondary tungsten plasma decreases from 100 eV to 2 eV during 100 μs [16]. The existence and influence of secondary plasma should be considered for samples irradiated within the PF-12 (sample distance from the anode 5.5–7.5 cm) as well as in the PF-1000. However, it should be noted that actual measurements of the duration of the pulses and other parameters of secondary plasma were not carried out during the experiments performed with the PF-12 device.

Although the influence of both off-normal events and steady-state or near steady-state plasma loads may lead to development of critical damages, the exact opposite might occur – the covering of cracks of material. Knowing such behaviour of the different tungsten alloys and grades is necessary for choosing the most suitable divertor material for fusion devices. Therefore, it is of interest to investigate the effect of consequent plasma pulses – how may the defects generated by one kind of pulses influence some other kind of defects that have occurred previously on the same surface.

To understand the combined influence of different power flux densities, experiments were carried out with using both very high power flux densities (PF-12) and also lower power flux densities (QSPA Kh-50). To achieve such treatment, the samples were irradiated by PF-12 with 100 deuterium plasma pulses at first. After that, two samples were irradiated by QSPA Kh-50 with 10 hydrogen plasma pulses. As the characteristics of QSPA plasma stream differ from the parameters of the plasma from PF-12, the characteristics of QSPA's plasma should be noted. The ion impact energy was ca. 0.4–0.6 keV, the maximum plasma pressure 0.32 MPa and stream diameter ca. 18 cm. The heat load of plasma was 90 J/cm^2 (as measured with a calorimeter) and exceeded the melting threshold for tungsten, which was experimentally shown in this facility to be of about 45 J/m^2. A hydrogen-plasma pulse shape was approximately triangular, and the pulse duration was ca. 0.25 ms (see [1] for detailed experimental set-up and device parameters). Garkusha *et al*. have shown that (a) irradiation of cracked tungsten causes the appearance of tungsten dust from intersections of the cracks [1], (b) the molten layer generated by plasma may lead to covering and disappearance of cracks, microcracks and to smoothing of a surface layer [20].

The surfaces and cross-sections of the irradiated samples were analysed by SEM and optical microscopy. Also, a 3D measurement of microroughness was carried out by a Bruker 3D white-light Optical Microscope Contour GT-K (at vertical resolution <0.01 nm, lateral resolution 0.38 μm, and single image resolution 1280 × 960 pixels). The amplitude parameters of 3D microroughness measurements were based on overall heights. The results include the root-mean-square of height distribution, skewness (or the degree of asymmetry of a surface height distribution), the degree of peakedness of a surface height distribution (or kurtosis) and an average of the highest and lowest points.

To estimate the damages in bulk, electrical conductivity was measured. This was carried out by the National Standard Laboratory for Electrical Quantities, using the electrical conductivity etalons set NPL no. 178 and the eddy current instrument Sigmatest 2.069, which enables to measure conductivity of non-ferromagnetic metals [21]. During the measurements, the conductivity was determined at the centre of the damaged area of each sample. The frequencies used during the measurements were 60, 120, 240, 480 and 960 kHz. The results were reduced to be in accordance with temperature of 20°C.

In all the experiments, polished double-forged tungsten (DFW) samples of dimensions (12 × 12 × 5) mm^3 were used as targets. The material was prepared for experiments by PLANSEE and supplied by IAEA (International Atomic Energy Agency) for Round-Robin tests in different facilities. DFW is of an interest as the grains of DFW have an elongated structure due to the forging process (see e.g. [11] for description of material manufacturing).

The detailed irradiation conditions as well as some results are given in Table 1. One should note that the data considering the samples DFW87 and DFW88 appear in Table 1 on two occasions, as they have been irradiated several times. In the rows where samples' names end with letter (a) , the samples were irradiated in the PF-12. In the rows where the names end with letter (b), the samples received additional irradiation in the QSPA Kh-50.

Table 1. Irradiation conditions, results measurements of cell's sizes and average microroughness of samples

No. of sample	Device	No. of pulses	Power flux density of plasma q_{pl} [MW/cm^2]	Duration of plasma flow q_{pl} [μs]	Power flux density of fast ions q_{ion} [MW/cm^2]	Duration of fast ions' flow q_{ion} [μs]	Size of macrocells [μm]	Size of microcells [μm]	Microroughness R_a [μm]
DFW 85	PF-12	25	50 (in zone B)	0.1	5×10^5	0.03	500 ± 91	23 ± 4	1.2 (max. 15.1)
DFW 86	PF-12	25	500 (in zone A)	0.05	5×10^4	0.01–0.02	365 ± 25	Not visible	1.8 (max. 9.0)
DFW 87a	PF-12	100	500 (in zone A)	0.05	5×10^4	0.01–0.02	378 ± 41	103 ± 16	5.4 (max. 47)
DFW 88a	PF-12	100	50 (in zone B)	0.1	5×10^5	0.03	189 ± 10	27 ± 1.5	5.1 (max. 55)
DFW 87b	QSPA Kh-50	10	0.36	250	–	–	329 ± 19	42 ± 4	2.5 (max. 9.5)
DFW 88b	QSPA Kh-50	10	0.36	250	–	–	215 ± 44	25 ± 5	9.6 (max. 36)
DFW 2	PF-1000	2	10^3 – 10^4	0.1	10^5 to 10^6	0.05	1450 ± 120	9 ± 2	Not measured
DFW 3	PF-1000	4	10^3 – 10^4	0.1	10^5 to 10^6	0.05	600*	–	Not measured

* Estimation of two cells.

Experimental results

Results and analysis of surface defects

The irradiated surfaces were investigated by SEM and an optical microscope. Although numerous images were obtained during the study, only a number of images are presented. DFW samples irradiated at different PF devices are shown in Fig. 2. For a comparison of surface defects, three samples are given: (a) DFW 87a (Figs. 2a, 2c – the magnifications on images are 50× and 200×, respectively), (b) DFW 88a (Figs. 2b, 2d – the magnifications on the images are 200× and 1000×, respectively; some specific defects, i.e. droplets and craters, are also indicated on the latter image), (c) DFW 2 (Fig. 2e), (d) DFW 3 (Fig. 2f). The results of measurements of microroughness and cell sizes are given in Table 1.

In Table 1, a macrocell is defined as an area bordered by so-called macrocracks (with width up to 2 μm) and a microcell is an area bordered with microcracks (with width of about 10–50 nm). For a comparison, one can see also Fig. 2b.

It was observed that all samples have practically identical damage features: wave-like structures, micro- and macrocracks formation, pores, etc. Though a density of different kind of damages (i.e. a ratio of the total area of specific defects to the total area of the investigated surface, determined by SEM images) depends strongly on plasma and ion flow power flux density. It can be seen that high heat loads result in droplets formation (and possible ejection) from the tungsten's surface with the simultaneous movement of the molten layer (see Figs. 2d and 2e). Closer exploration of SEM images shows that droplets are located next to grooves, holes (Figs. 2b, 2d) or cracks (Fig. 2e), so the droplets should have been emanated from the same grooves or cracks.

In Table 1, the sizes of cells, as measured from SEM images (see Fig. 2b), are presented. These cells sizes are defined as average cell diameters. Also, the average microroughness R_a of each sample is indicated. This parameter has been measured along crossed lines over the investigated surface. The maximum roughness is also shown, being a difference between the lowest and the highest points. It should be noted that the average roughness of a polished sample before irradiation was 0.33 μm and the maximum was 5.2 μm.

Plasma-material interaction studies showed that higher heat flux factor F leads to higher values of microroughness upon irradiated surfaces (see [1, 9, 10, 22]). Therefore, the sample DFW 87a should have greater microroughness R_a values than DFW 88a. Though the difference between the values of R_a for samples DFW 87a and 88a is small (about 5–6%), the density of cracks is bigger in the case of DFW 88a. Examination of SEM images at higher magnification (Fig. 2c) reveals that there exists a mesh of microcracks, with almost no visible separating lines between the cells. This allows to suspect that secondary tungsten plasma has covered the microcracks. The same phenomenon is valid for cells' mesh development on the sample irradiated within PF-1000, also.

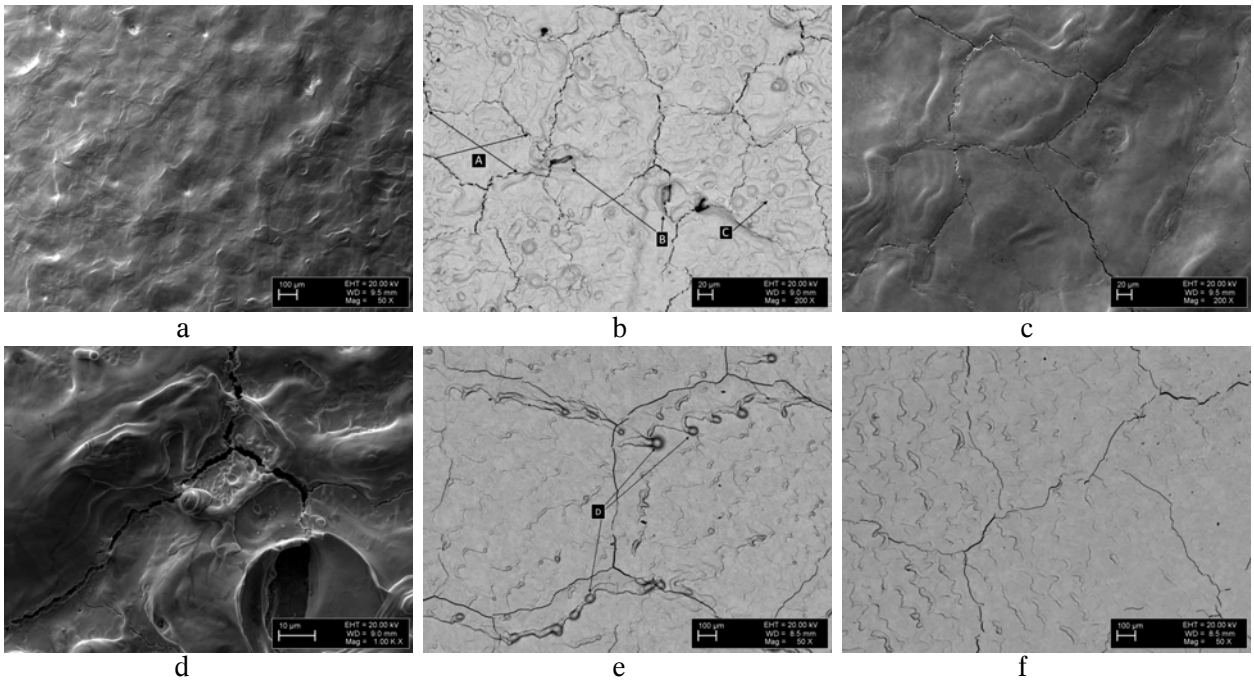

Fig. 2. Scanning electron microscope and optical microscope images of DFW samples: (a and c) DFW 87a (PF-12, zone A, 100 pulses); (b and d) DFW 88a (PF-12, zone B, 100 pulses); (e) PF-1000, 4 pulses; (f) PF-1000, two pulses. Notations: A – macrocells between macrocracks, B – craters, C – microcells between microcracks, D – droplets.

For samples that have either been (a) with small number of shots – DFW 2 and 3 or (b) with powerful ion beams – DFW 86 and 87a (in which case there is a cracks covering effect of secondary plasma) – the microcells' size is above 25 mm (44–55 μm). With either (c) increasing number of shots or (d) irradiating the sample in QSPA Kh-50 – i.e. in DFW 87b and 88b, the size of microcells is reduced. On the other hand, when a mesh of microcracks was developed during plasma pulses at PF-12, which were followed by irradiation of the sample in QSPA Kh-50 (with much smaller values of power flux density), no significant change of micro- or macrocells' sizes was observed. For a comparison, when tungsten was produced by usual rolling and single forging technology, the mesh of microcracks occurred on the samples already after eight shots of plasma [9, 10].

Experiments carried out by QSPA Kh-50 have shown that generation of molten layer leads also to emission of droplets and therefore to the appearance of tungsten dust. Thus, as density of cracks on DFW 88a is greater than on DFW 87a, also, the

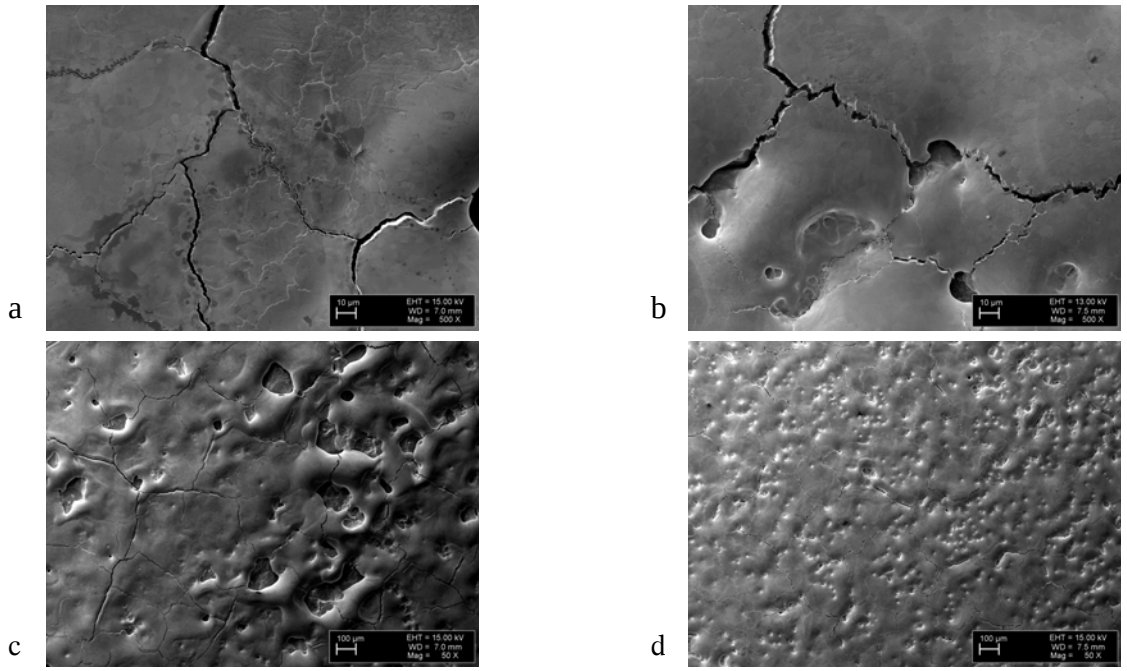

Fig. 3. (a and c) DFW 88b samples irradiated by 100 pulses within the PF-12, at $q = 500$ MW/cm^2 and afterwards by 10 pulses within the QSPA Kh-50, at $Q = 90$ J/cm^2; (b and d) DFW 87b samples irradiated by 100 pulses within the PF-12, at $q = 50$ MW/cm^2 and afterwards by 10 pulses within the QSPA Kh-50, at $Q = 90$ J/cm^2.

characteristic defects on the samples are different (there are droplets, groves and craters on DFW 88a). This leads to generation of more groves, holes and macrocracks on DFW 88b (see Fig. 3a, 3c). This may be the main reason for the increase of the average microroughness of a sample (sample DFW 88b in Table 1). As seen from Fig. 3b and 3d, the sample DFW 87b has more pronounced defects on the bigger scale (Fig. 3d), but the surface between bigger holes and craters is in general smoother (lack of small holes and groves). This may be the reason for smaller microroughness of the sample DFW 87b – the density and character of defects on DFW 87b is different in comparison with DFW 88b.

After irradiation of both samples on QSPA Kh-50 (DFW 87b and 88b) with hydrogen plasma flows and lower power flux densities, an increase of apparent melting traces occurs (Figs. 3a and 3b). On the other hand, when comparing the samples in microscale, the damages of both samples are quite similar (see Figs. 3a and 3b). Though the mesh of microcracks has developed more on the sample, which was more damaged previously (DFW 88a).

In conclusion, the initial cracks mainly will deteriorate – all cracks will widen and new defects will be generated upon the older ones. On the other hand, on the sample, which initially had a rather damaged surface, the additional irradiation of the sample in QSPA Kh-50 diminished the prominence of droplets and caverns on the surface, leading thus to a smoother surface, which means that the number of holes per investigated area decreases (though an average area of the holes increases) (see also Fig. 4).

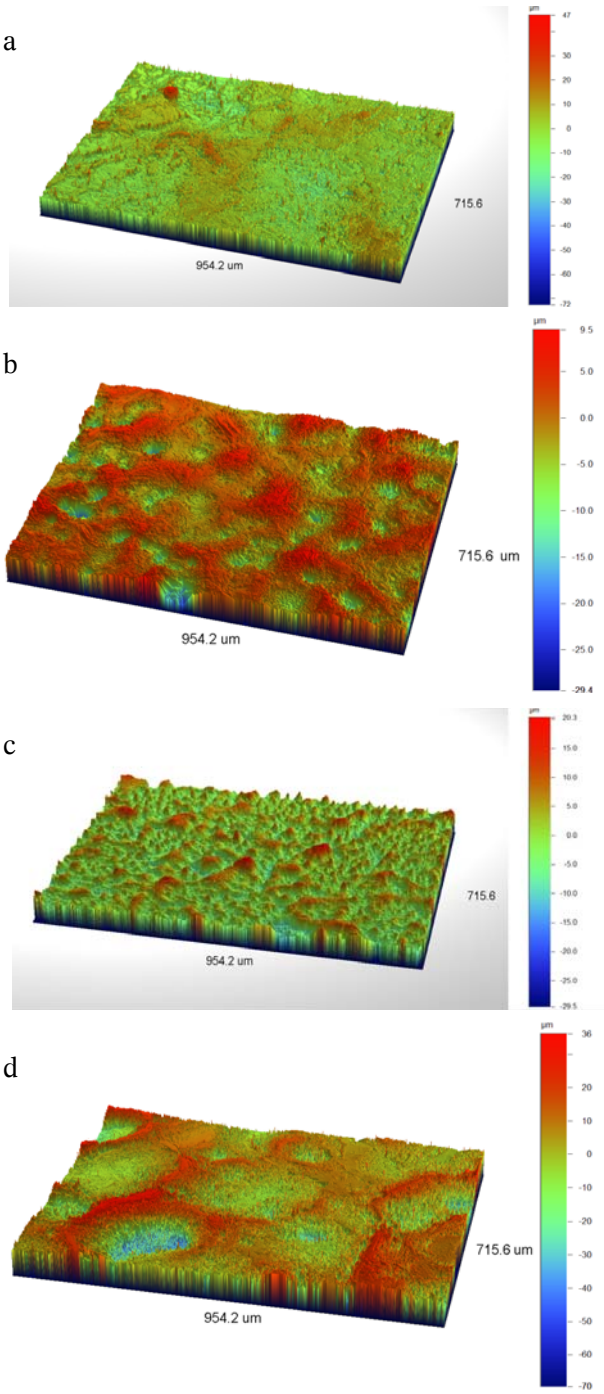

Fig. 4. Microroughness of DFW samples irradiated by 100 plasma-ion pulses at the PF-12 device, as measured before (samples with letter a) and after (samples with letter b) their irradiation at the QSPA Kh-50 facility. From top: (a) DFW 87a, (b) DFW 87b, (c) DFW 88a, (d) DFW 88b.

Results and analysis of bulk effects

To estimate the depth of damaged layer, a non-destructive method of measurement of electrical conductivity was used on DFW samples. It is known that conductivity of solid material depends on concentration of point defects, microcracks and other occurring bulk defects. The results of the analysis can be seen in Fig. 5.

Initially, the conductivity of the material was 18 MS/m and did not depend on depth. The results indicate that depth of damaged layer is, in general, in correlation with the power flux density values of plasma and fast ions. Dependence on the number of pulses is rather weak. Cooperative experiments with team of the Institute of Plasma Physics and Laser Microfusion have shown that powerful ion beams generate shock waves penetrating into material and also through thin materials. This phenomenon was also theoretically shown by Latyshev from A. A. Baikov Institute of Metallurgy and Material Sciences.

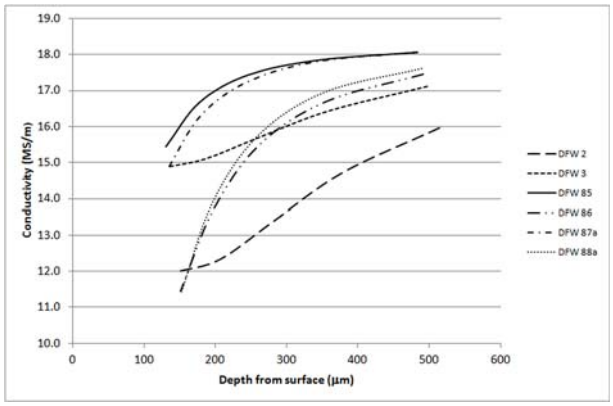

Fig. 5. Dependence of conductivity σ on depth from surface δ. It should be noted that usually the penetration depth equal to 3δ is considered.

Computations by Latyshev *et al*. have shown that the pressure of the shock wave can reach 20 GPa in the bulk. It can go as deep as 500–800 μm inside the bulk, depending on the initial power flux density of fast ions on the samples' surface [23].

When comparing the results of conductivity of samples that have been irradiated in the same device and conditions varying only the by number of pulses, the results indicate that the average influence of fast ions during each pulse does not vary greatly and the cumulative effect of pulses is weak. Nevertheless, powerful ion beams (penetrating into the material) can generate damages in the bulk, even in cases when the surface damages are inessential (see samples DFW 87a and 88a, Figs. 2a, 2c and 5).

Discussion

Research on the interaction between hot dense deuterium plasma and double forged tungsten samples has been carried out at PF-1000, PF-12 and QSPA Kh-50. In case of dense plasma focus devices, the duration of plasma pulses τ is much shorter and the power flux density q is much higher than the values calculated for VDEs, ELMs and disruptions for ITER. The heat load factor $F = q \cdot \tau^{1/2}$ calculated for abovementioned events is approximately the same as reached using PF devices. Heat damage factor of plasma flow generated by PF-12 allows simulating all the off-normal events in ITER: ELMs, VDEs and disruptions. Effects of generated by PF-1000 are more similar to VDE and disruptions effects in ITER. Plasma generator QSPA Kh-50 generates ELM-like plasma. Ion flows generated by PF-12 and specifically by PF-1000 allow simulating conditions in DEMO or inertial fusion devices. Thus, simulation of plasma and ion flows by plasma-focus devices PF-12 and PF-1000, and plasma generator QSPA Kh-50 allows modelling the conditions not only for ITER, but also for other fusion devices.

The results indicate that the investigated materials showed practically the same kind of damages, such as melted layer, pores and meshes of cracks. However, in case of big number of plasma pulses, the appearance of bubbles, which will eventually burst and therefore craters will appear, can be seen. It was found that the increasing number of plasma pulses (from 25 to 100) leads to decrease of sizes of macrocells as well as microcells. The research shows that for these experiments with DFW under the same conditions (PF-12), the size of microcells closes to 25 μm, which is larger than in case of single forged tungsten (W) and tungsten doped with 1% lanthanum-oxide (WL10) [9]. Also, it should be noted that development of mesh of cracks (mesh of cells) took two to eight plasma pulses for single forged W and WL10 [10]. During the previous ITER-related studies considering tungsten (DFW and ultra-pure tungsten) grades, the samples were irradiated with either laser, plasma (in tokamak GlobusM and QSPA Kh-50) or electrons (JUDITH) pulses with ELM-related heat load factors [1, 5, 11, 20, 24]. The results concerning surface defects and their development during the increase of particle pulses are similar to those obtained in this study. Namely, the generation of macro- and microcracks and decrease of cells' average sizes after irradiation with multiple particle fluxes' pulses (100 pulses and more). Though the influence of laser and electron beams is mainly due to heating and generation of thermal stresses, which lead to development of cracks. The results indicate that irradiation of DFW with deuterium plasma and fast deuterons may generate bubbles, which eventually may lead to bursting of bubbles and therefore to craters (which later become the sources of tungsten dust).

Irradiation of such damaged samples with plasma of lower power flux density (with heat load factor values exceeding the melting threshold) by QSPA Kh-50 leads only to the smoothing of surface but does not change mesh of cracks significantly. The effect of plasma fluxes with the heat load factors below melting threshold should be investigated in the future to obtain more information on the development of mesh of cracks and other defects.

Damages in bulk of material were investigated by conductivity measurements. The analysis revealed that a decrease in conductivity is correlated with the power flux density of plasma (in case of 100 plasma pulses). However, the results do not indicate clearly, whether the decrease in conductivity is due to a heat load on the surface or an effect caused by fast ion fluxes. A decrease in conductivity is influenced by surface and bulk factors. A surface factor of the conductivity's decrease occurs due to changes of surface layer's structure after melting, re-crystallisation and generation of surface defects (pores, droplets, etc). A bulk factor is related to generation of dislocations and point defects (vacancies, Frenkel pairs, impurities), weakening of bonds between grains, but also re-crystallisation in the solid phase, due to a cooperative effect of shock wave and heating--cooling cycles.

Investigation of bulk defects in tungsten by cross-sections (on samples those have been irradiated without powerful ion fluxes) has revealed the occurrence of re-crystallisation and development of subgrains in depth of about 100 μm and less [1, 20, 24]. On the other hand, a decrease in materials' microhardness in a cross-section has been observed in both single-forged tungsten samples, as well as in WL10 [10] irradiated within the PF-12 with plasma incorporated with fast (100 keV) ion fluxes. Depending on the material, the values vary within 250–500 μm. As it was shown theoretically by Latyshev *et al*. [23], the shock wave can reach as deep as 500–800 μm. Thus, it can be concluded that a decrease in conductivity is due to integral changes of materials state, which depend on irradiation conditions, development and a propagation of shock wave, but also on re-crystallisation processes of the material. One can conclude that microstructure of the subsurface layer (up to 500 μm) has changed. Though, the nature of the decrease in conductivity and effects of different processes on it should be investigated more thoroughly.

Conclusions

The most important results can be summarised as follows:

1. The irradiation of double-forged tungsten with ELM-related heat-load plasma fluxes leads to generation and development of micro- and macrocracks. Though it should be mentioned that the cell sizes occurring in the DFW's mesh of cracks are larger than in a case of either single--forged tungsten or tungsten doped with 1% lanthanum-oxide. Therefore, the probability of generation of a tungsten dust and/or melting traces, by plasma pulses with heat load factors below melting threshold, is smaller than in case of single-forged tungsten.
2. A comparison with previous research on single--forged tungsten and tungsten dispersed with lanthanum oxide [9, 10] shows that double forging of tungsten has led to improvement of the materials properties, namely strengthening of binding between grains. Thus, for the development of a mesh of cracks more powerful plasma pulses are needed.
3. In comparison to the earlier studies of single--forged tungsten and WL10 [9, 10] samples, the decrease of generated droplets on DFW samples, as estimated by SEM images, is noteworthy.
4. Considering the fact that dispersing tungsten with oxides has led to the decrease of brittleness, it can be concluded that future research should explore the prospects of using multiple-forged alloys of tungsten as a possible material for diverters in fusion facilities.
5. A comparison of defects, which are produced by different particle generators (lasers, plasma generators, electron accelerators) upon the same tungsten grades, shows similarity of surface defects and similar behaviour of the tungsten samples. This allows to suggest that the results gained by PF devices with very powerful, but short plasma-ions pulses (with high heat load factors) are valid for ITER-related off-normal events calculated with much lower power flux densities and much longer plasma pulses.
6. The reported study has shown that, besides of similar effects on DFW samples due to heat load generated by different particle loads, there are important differences, as appearance of bubbles when using PF-devices. Therefore, in the future also research using helium, and deuterium with different particle energies, should be carried out.

Acknowledgments. This work was supported by European Social Fund's Doctoral Studies and Internationalisation Programme DoRa, which is carried out by Foundation Archimedes, Estonian Science Foundation – Estonia grant no. ETF9005, by the International Atomic Energy Agency CRP grant nos. RC-16931, RC--16932, RC-16954, RC-16955, RC-16956, RC-16960, and by the European Union through the Regional Development Fund (Centre of Excellence 'Mesosystems: Theory and Applications', TK114).

This work was performed at the Tallinn University, Estonia, and the IPPLM, Poland.

References

1. Garkusha, I. E., Makhlaj, V. A., Aksenov, N. N., Byrka, O. V., Malykhin, S. V., Pugachov, A. T., Bazylev, B., Landman, I., Pinsuk, G., Linke, J., Wirtz, M., Sadowski, M. J., & Skladnik-Sadowska, E. (2015). High power plasma interaction with tungsten grades in ITER relevant conditions. *J. Phys. Conf. Ser*., *591*, 012030.
2. Rieth, M., Dudarev, S. L., Gonzales de Vicente, S. M., Aktaa, J., Ahlgren, T., Antusch, S., Armstronga, D. E. J., Balden, M., Baluc, N., Barthe, M. -F., Basuki, W. W., Battabyal, M., Becquart, C. S., Blagoeva, D., Boldyryeva, H., Brinkmann, J., Celino, M., Ciupinski, L., Correia, J. B., De Backer, A., Domain, C., Gaganidze, E., Garcia-Rosales, C., Gibsona, J., Gilbert, M. R., Giusepponi, S., Gludovatz, B., Greuner, H., Heinola, K., Höschen, T., Hoffmann, A., Holstein, N., Koch, F., Krauss, W., Li, H., & Lindig, S. (2013). A brief summary of the progress on the EFDA tungsten materials program. *J. Nucl. Mater*., *442*(Suppl. 1), S173–S180.
3. Hirai, T., Escourbiac, F., Carpentier-Chouchana, S., Fedosov, A., Ferrand, L., Jokinen, T., Komarov, V., Kukushkin, A., Merola, M., Mitteau, R., Pitts, R. A., Shu, W., Sugihara, M., Riccardi, B., Suzuki, S., & Villari, R. (2013). ITER tungsten divertor design development and qualification program. *Fusion Eng. Des.*, *88*, 1798–180.
4. Pitts, R. A., Carpentier, S., Escourbiac, F., Hirai, T., Komarov, V., Kukushkin, A. S., Lisgo, S., Loarte, A., Merola, M., Mitteau, R., Raffray, A. R., Shimada, M., & Stangeby, P. C. (2011). Physics basis and design of the ITER plasma-facing components. *J. Nucl. Mater*., *415*, S957–S964.
5. Cicuttin, A., Crespo, M. L., Gribkov, V. A., Niemela, J., Tuniz, C., Zanolli, C., Chernyshova, M., Demina, E. D., Latyshev, S. V., Pimenov, V. N., & Talab, A. A. (2015). Experimental results on the irradiation of nuclear fusion relevant materials at the dense plasma focus 'Bora' device. *Nucl. Fusion*, *55*(6), 063037.
6. Lemahieu, N., Linke, J., Pintsuk, G., Van Oost, G., Wirtz, M., & Zhou, Z. (2014). Performance of yttrium doped tungsten under 'edge localized mode'-like loading conditions. *Phys. Scr., T159*, 014035.
7. Linke, J., Loewenhoff, T., Massaut, V., Pintsuk, G., Ritz, G., Rödig, M., Schmidt, A., Thomser, C., Uytdenhouwen, I., Vasechko, V., & Wirtz, M. (2011). Performance of different tungsten grades under transient thermal loads. *Nucl. Fusion*, *51*, 073017.
8. Qu, S., Gao, S., Yuan, Y., Li, C., Lian, Y., Liu, X., & Liu, W. (2015). Effects of high magnetic field on the melting behavior of W-1wt%La_2O_3 under high heat flux. *J. Nucl. Mater*., *463*, 189–192.
9. Shirokova, V., Laas, T., Ainsaar, A., Priimets, J., Ugaste, U., Väli, B., Gribkov, V. A., Maslyaev, S. A., Demina, E. V., Dubrovsky, A. D., Pimenov, V. N., Prusakova, M. D., & Mikli, V. (2014). Armor materials' behavior under repetitive dense plasma shots. *Phys. Scr., T161*, 014045.
10. Shirokova, V., Laas, T., Ainsaar, A., Priimets, J., Ugaste, U., Demina, E. V., Pimenov, V. N., Maslyaev, S. A., Dubrovsky, A. V., Gribkov, V. A., Scholz, M., & Mikli, V. (2013). Comparison of damages in tungsten and tungsten doped with lanthanum-oxide exposed to dense deuterum plasma shots. *J. Nucl. Mater*., *435*, 181–188.

11. Huber, A., Arakcheev, A., Sergienko, G., Steudel, I., Wirtz, M., Burdakov, A. V., Coenen, J. W., Kreter, A., Linke, J., Mertens, Ph., Philipps, V., Pintsuk, G., Reinhart, M., Samm, U., Shoshin, A., Schweer, B., Unterberg, B., & Zlobinski, M. (2014). Investigation of the impact of transient heat loads applied by laser irradiation on ITER-grade tunsgten. *Phys. Scr., T159*, 014005.
12. Sheng, H., Van Oost, G., Zhurkin, E., Terentyev,, D., Dubinko, V. I., Uytdenhouwen, I., & Vleugels, J. (2014). High temperature strain hardening behavior in double forged and potassium doped tungsten. *J. Nucl. Mater.*, *444*, 214–219.
13. Fujitsuka, M., Shinno, H., Tanabe, T., & Shiraishi, H. (1991). Thermal shock experiments for carbon materials by electron beams. *J. Nucl. Mater.*, *17A*, 189–192.
14. Riccardo, V., Loarte, A., & JET EFDA Contributors. (2005). Timescale and magnitude of plasma thermal energy loss before and during disruptions in JET. *Nucl. Fusion*, *45*, 1427–1438.
15. Bernard, A., Bruzzone, H., Choi, P., Chuaqui, H., Gribkov, V., Herrera, J., Hirano, K., Krejci, A., Lee, S., Luo, C., Mezzetti, F., Sadowski, M., Schmidt, H., Wone, K., Wang, C. S., & Zoita, V. (1998). Scientific status of plasma focus research. *J. Moscow Phys. Soc.*, *8*, 93–170.
16. Gribkov, V. A. (2015). Physical processes taking place in dense plasma focus devices at the interaction of hot plasma and fast ion streams with materials under test. *Plasma Phys. Contr. Fusion*, *57*, 065010.
17. Pimenov, V. N., Demina, E. V., Maslyaev, S. A., Ivanov, L. I., Gribkov, V. A., Dubrovsky, A. V., Ugaste, U., Laas, T., Scholz, M., Miklaszewski, R., Kolman, B., & Tartari, A. (2008). Damage and modification of materials produced by pulsed ion and plasma streams in Dense Plasma Focus device. *Nukleonika*, *53*(3), 111–121.
18. Gribkov, V. A., Banaszak, A., Bienkowska, B., Dubrovsky, A. V., Ivanova-Stanik, I., Jakubowski, L., Karpinski, L., Miklaszewski, R. A., Paduch, M., Sadowski, M. J., Scholz, M., Szydlowski, A., & Tomaszewski, K. (2007). Plasma dynamics in the PF-1000 device under full-energy storage: II. Fast electron and ion characteristics versus neutron emission parameters and gun optimization perspectives. *J. Phys. D-Appl. Phys.*, *40*, 3592–3607.
19. Gribkov, V. A., Bienkowska, B., Borowiecki, M., Dubrovsky, A. V., Ivanova-Stanik, I., Karpinski, L., Miklaszewski, R. A., Paduch, M., Scholz, M., & Tomaszewski, K. (2007). Plasma dynamics in PF-1000 device under full-scale energy storage: I. Pinch dynamics, shock-wave diffraction, and inertial electrode. *J. Phys. D-Appl. Phys.*, *40*, 1977–1989.
20. Makhlaj, V. A., Garkusha, I. E., Aksenov, N. N., Bazylev, B., Landman, I., Linke, J., Malykhin, S. V., Pugachov, A. T., Sadowski, M. J., Skladnik-Sadowska, E., & Wirtz, M. (2014). Tungsten damage and melt losses under plasma accelerator exposure with ITER ELM relevant conditions. *Phys. Scr., T159*, 014024.
21. Pokatilov, A., Parker, M., Kolyshkin, A., Märtens, O., & Kübarsepp, T. (2013). Inhomogeneity correction in calibration of electrical conductivity standards. *Measurement*, *46*, 1535–1540.
22. Gribkov, V. A., Paduch, M., Zielinska, R., Laas, T., Shirokova, V., Väli, B., Paju, J., Pimenov, V. N., Demina, E. V., Latyshev, S. V., Niemela, J., Crespo, M. -L., Cicuttin, A., Talab, A. A., Pokatilov, A., & Parker, M. (2015). Parallel investigation of double forged pure tungsten samples irradiated in three DPF devices. *J. Nucl. Mater.*, *463*, 341–346.
23. Latyshev, S. V., Gribkov, V. A., Maslyeav, S. A., Pimenov, V. N., Paduch, M., & Zielinska, E. (2015). Generation of shock waves in materials science experiments with dense plasma focus device. *Inorg. Mater.-Appl. Res.*, *6*(2), 91–95.
24. Ankudinov, A. V., Voronin, A. V., Gusev, V. K., Gerasimenko, Ya. A., Demina, E. V., Prusakova, M. D., & Sud'enkov, Yu. V. (2014). Influence of a plasma jet at different types of tungsten. *Techn. Phys.*, *59*, 346–352.